

PAPER • OPEN ACCESS

Investigation of room temperature multispin-assisted bulk diamond ^{13}C hyperpolarization at low magnetic fields


To cite this article: Ralf Wunderlich *et al* 2018 *J. Phys.: Condens. Matter* **30** 305803

View the [article online](#) for updates and enhancements.

You may also like

- [Electrical activity of ON and OFF retinal ganglion cells: a modelling study](#)
Tianruo Guo, David Tsai, John W Morley et al.
- [Modelling the visual response to an OUReP retinal prosthesis with photoelectric dye coupled to polyethylene film](#)
Koichiro Yamashita, Prathima Sundaram, Tetsuya Uchida et al.
- [High-field small animal magnetic resonance oncology studies](#)
Louisa Bokacheva, Ellen Ackerstaff, H Carl LeKaye et al.

Investigation of room temperature multispin-assisted bulk diamond ^{13}C hyperpolarization at low magnetic fields

Ralf Wunderlich¹ , Jonas Kohlrautz¹, Bernd Abel², Jürgen Haase¹ and Jan Meijer¹

¹ Faculty of Physics and Earth Sciences, Felix Bloch Institute for Solid State Physics, Leipzig University, Linnstrassé 5, 04103 Leipzig, Germany

² Leibniz-Institute of Surface Engineering (IOM), Permoserstrasse 15, 04318 Leipzig, Germany

E-mail: ralf.wunderlich@uni-leipzig.de

Received 14 March 2018, revised 7 June 2018

Accepted for publication 13 June 2018


Published 4 July 2018



Abstract

In this work we investigated the time behavior of the polarization of bulk ^{13}C nuclei in diamond above the thermal equilibrium. This nonthermal nuclear hyperpolarization is achieved by cross relaxation between two nitrogen related paramagnetic defect species in diamond in combination with optical pumping. The decay of the hyperpolarization at four different magnetic fields is measured. Furthermore, we use the comparison with conventional nuclear resonance measurements to identify the involved distances of the nuclear spin with respect to the defects and therefore the coupling strengths. Also, a careful look at the linewidth of the signal give valuable information to piece together the puzzle of the hyperpolarization mechanism.

Keywords: nuclear hyperpolarization, NV center, diamond

 Supplementary material for this article is available [online](#)

(Some figures may appear in colour only in the online journal)

Introduction


Any spin resonance technique, including nuclear magnetic resonance (NMR), is based on the occupation difference of the energy levels associated with different magnetic quantum numbers at a given magnetic field. Unfortunately, this is given by the Boltzmann distribution and leads to a tiny occupation difference at room temperature. In recent years, more and more experimental as well as theoretical contributions are published in the literature dealing with nuclear hyperpolarization utilizing the negatively charged nitrogen vacancy (NV) center in diamond [1–9]. Recently, a nuclear hyperpolarization method without the need of microwave application was presented

[10, 11]. There, it is shown that cross relaxation (CR) between NV centers and substitutional nitrogen (P1) centers leads to a ^{13}C hyperpolarization in several narrow magnetic field regions in the range of 48.5–53.5 mT. An additional advantage of this technique is the applicability of type I diamonds without the need of ultra pure and expensive samples. Here, we investigate the time dynamics of this method. Furthermore, a comparison of hyperpolarized signals with conventional measurements in the thermodynamic equilibrium (TE) will be used to identify the polarised regions with respect to the paramagnetic defects.

Results

Time dependence of nuclear hyperpolarization

The experimental setup for the hyperpolarization measurements is described in detail in [10]. We used a single crystal

 Original content from this work may be used under the terms of the [Creative Commons Attribution 3.0 licence](#). Any further distribution of this work must maintain attribution to the author(s) and the title of the work, journal citation and DOI.

diamond sample with an estimated nitrogen content of 200 ppm, primarily present as P1 centers. The NV density is estimated to be maximal in the range of several ppm. The crystallographic [111] direction of the diamond sample was set parallel to the external magnetic field. All nuclear free induction decay (FID) signals were recorded at 7.05 T (300 MHz proton Larmor frequency), if not described differently. The advantage of using bulk NMR techniques in comparison to optically detected magnetic resonance (ODMR) is that this technique is sensitive to all nuclear spins, even if they are far away from any ODMR active center.

In the following, we present the characteristic build up time as well as the decay time at four different magnetic fields of the nuclear hyperpolarization. For the build up time measurement, the sample was exposed to a 5W laser light at 532 nm for varying illumination times at a magnetic field of about 49.5 mT. This corresponds to the magnetically first resonant CR between parallel aligned NV centers and P1 centers which are oriented in an angle of 109° (figure 1(b)). After the illumination the sample was transferred into the NMR probe at 7.05 T and a $\pi/2$ pulse was applied immediately. Figure 1(a) shows the average over three runs of this procedure per illumination time. The characteristic pumping time in this experiment was determined to about $T_{\text{pump}} = 102(14)$ s. In addition, the linewidth (full width at half maximum (FWHM)) of the Fourier transformed NMR signal was analyzed and the values are given in the inset of figure 1(a) and scatter around 200 kHz. Due to low signal to noise (SNR) ratios for short illumination times, two types of evaluations were performed: first, the FWHM value of the linearly interpolated raw data and second the value extracted from a fit of two Gaussian (for details see supplemental material³).

Another important parameter is the typical depletion time of the hyperpolarization signal. For this reason, we measure the decay time at four characteristic magnetic fields, namely slightly below, exactly at, slightly above and far above the resonant spin polarization transfer magnetic field. The polarization procedure for each experiment takes place at the indicated field point in figure 1(b), where also the pumping time was investigated. The decay of the polarization was measured with a pumping time of 200 s to 250 s which is sufficient to be in the saturated region of the pumping process. Afterwards, the laser was switched off and the magnetic field was set to the selected value. The NMR measurement takes place after varying duration in this selected magnet field. The decay was fitted to an single exponential function. Within the accuracy of the measurement no significant change in the decay times was noticeable. The values range from 50 s to 80 s, in consideration of the uncertainty of the fits. This is about 2.5 times faster than the characteristic pumping time. A possible reason is discussed below. With increasing the magnetic field to 7.05 T there is a tremendous increase in the decay time by a factor of 200 with a time constant in the range of 2.5 h. Due to this long time, no change in the signal can be recognized within the first 300 s (figure 3(a)) and even an observation time over 200 min

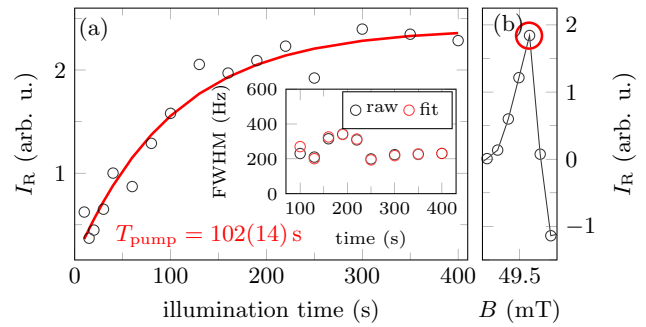


Figure 1. (a) Integral intensity of the real part of the Fourier transformed NMR signal (I_R) after different illumination times (5W, 532 nm). Red curve is a fitted exponential function (with time constant T_{pump}). The inset shows the corresponding linewidths of the spectra. All values are the average over 3 measurement runs. (b) Section of the magnetic field dependent hyperpolarization pattern after an irradiation time of 200 s. The red circle indicates the magnetic field, where the time dependent measurements were performed.

(figure 3(b)) identifies just a slow decrease of the signal. This decrease appears to be linear due to $\exp(-t) \approx 1 - t$. The extreme long T_1 time might be a manifestation of the wide off-resonant Zeeman splittings of the two defect systems and may be an advantage for future developments and novel applications.

For a proof of concept and as reliability check a series of solid echo measurements was conducted under hyperpolarization. This kind of pulse sequence is used to verify dipolar coupling of magnetically equivalent spin-1/2 pairs among themselves. After a specific delay time (in this case 0.5 ms) the first $\pi/2$ pulse is followed by a second one with a relative phase of $\pm 90^\circ$. The receiver phase is equal to that of the first pulse. The accumulated signal in the time domain over two full phase cycles (8 measurements per cycle) is shown in figure 4(a) and the corresponding pulse sequence is given in figure 4(c) and the table figure 4(b). The clear increase after 0.5 ms indicates a dipolar coupling of the hyperpolarized ^{13}C spin.

Thermal equilibrium NMR

In addition to the hyperpolarization measurements, conventional measurements in quasi thermal (QT) equilibrium were conducted in the very same setup. This means, the diamond was attached to the transfer shuttle but stays in the NMR probe in the center of the 7.05-T magnet. The absence of hyperpolarization and the long lattice relaxation time requires a large number of accumulations and causes a long measurement times. Standard FID measurements with different delay times between every sequence were performed. The linewidths of the NMR spectra are calculated as described above and shown in figure 5 (see supplemental material for raw data). With increasing delay time, the linewidth decreases and reaches a value around 300 Hz for a delay time of 4 h.

To improve the SNR and to investigate the nuclear spin system in more detail, we performed QT measurement in a 11.74-T magnet (500 MHz proton Larmor frequency) in combination with a Bruker Avance III HD spectrometer. The

³ See supplemental material at (stacks.iop.org/JPhysCM/30/305803/mmedia) for raw data and calculation of spin diffusion.

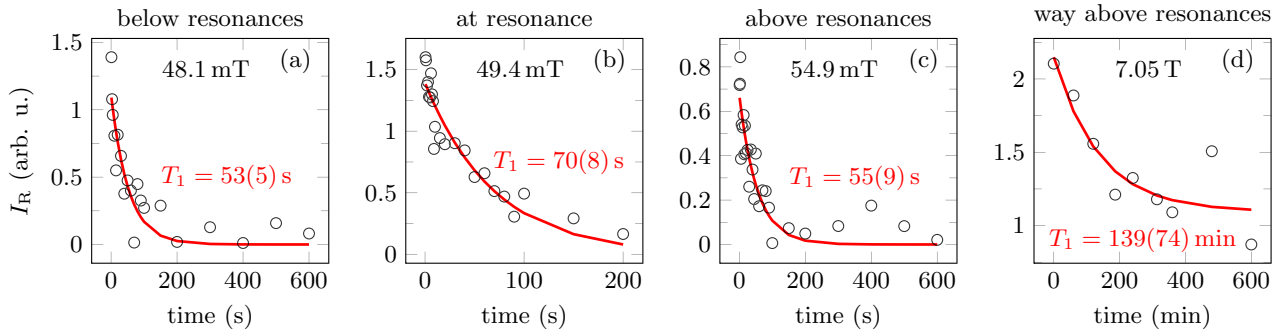


Figure 2. Specific decays of the hyperpolarization signal (integrated real part of the Fourier transform I_R) depending on the magnetic field after an illumination time of 200 s ((a), (c)) and 250 s (b) and (d), respectively (532 nm, 5 W). The polarization procedure for each experiment takes place at the indicated field point in figure 1(b), where the pumping time was investigated. The T_1 time in the 7.05 T field (c) is about 2.5(10) h and were measured with the same polarization conditions like in (b).

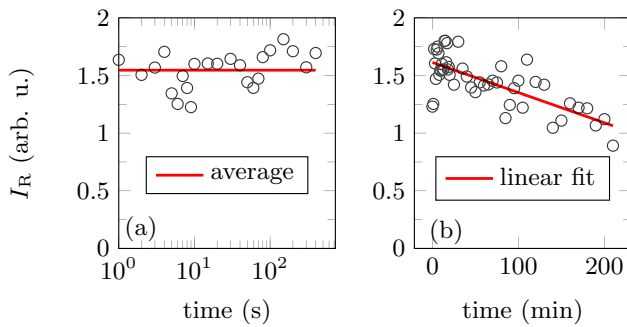


Figure 3. Time behavior of the hyperpolarization effect at the 7.05 T field within the first 400 s (a) and first 200 min (b) after shuttling (integrated real part of the Fourier transform I_R). In both cases each data point is averaged over three measurements.

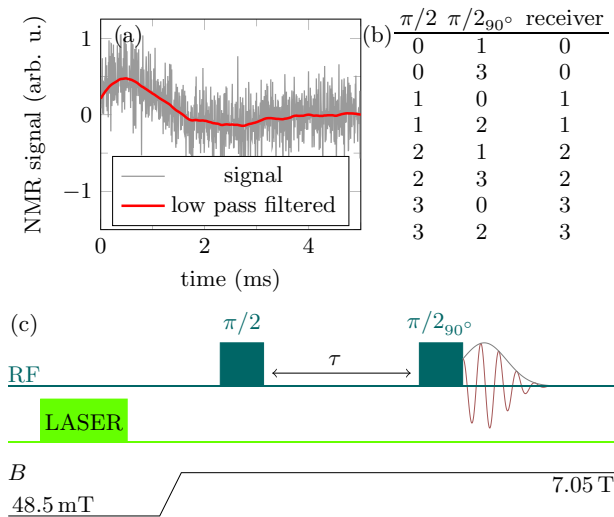


Figure 4. (a) The NMR signal of a hyperpolarized solid echo experiment with $\tau = 500 \mu\text{s}$ in the time domain (real part). (b) The table shows the phases of one phase cycle for the first and second $\pi/2$ pulse as well as the receiver phase. Here 0, 1, 2, 3 correspond to a phase of 0, $\pi/2$, π and $3\pi/2$. The signal in (a) is accumulated over two phase cycles. (c) Pulse sequence of the hyper polarized solid echo experiment.

diamond sample was placed in a HF coil with a quality factor of $Q \approx 190$ and was oriented with its crystallographic [1 1 1] direction parallel to the applied magnetic field. A carrier frequency of 125.758 189 MHz was used and the length for a $\pi/2$

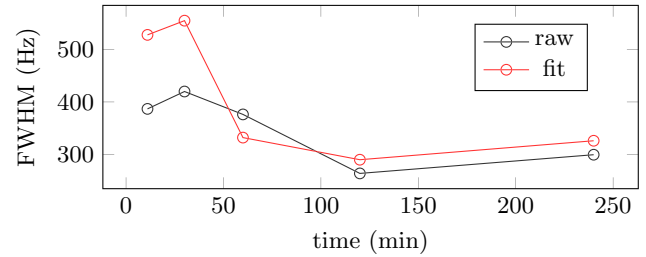


Figure 5. Extracted linewidths from non hyperpolarized measurements with different repetition times (11 min, 30 min, 1 h, 2 h, 4 h) corresponding to an accumulation of 267, 87, 38, 36 and 73 single measurements. Here, the repetition time is defined as the time between two measurement sequences, consisting of a $\pi/2$ pulse and a subsequent acquisition of the FID.

pulse was determined to be $5.5 \mu\text{s}$. The measurements were conducted as ‘saturation recovery’ with four $\pi/2$ pulses at the beginning of each measurement sequence, see figure 6(d). Figure 6(a) shows the increasing integral NMR signal for different delay times after die saturation pulses. For the first two data points (10 s, 30 s) 512 scans were accumulated, four scans for the data points from 10^2 s to 3×10^4 s and a single measurement for 26×10^4 s (≈ 3 d). The data is fitted to a double exponential function with a slow $S_s(t)$ and a fast component $S_f(t)$:

$$S(t) = S_s(t) + S_f(t) = A_s \cdot \left(1 - \exp\left(-\frac{t}{T_1^s}\right)\right) + A_f \cdot \left(1 - \exp\left(-\frac{t}{T_1^f}\right)\right).$$

The fit yields $T_1^s = 2.0(4)$ h and $T_1^f = 4.4(4)$ min, respectively.

A closer look at the peaks reveals a shifting of the center frequency as well as a narrowing of the peak width (figures 6(b) and (c)) with increasing delay time. Although the effect of shifting is rather small the line width (FWHM) decreases by 30% from 1.1 KHz to 0.8 KHz. This corroborates the trend of a decreasing linewidth with increasing repetition time of the QT measurement at 7.05 T.

Discussion

The results and in particular the comparison of hyperpolarized and QT measurements give evidence that the described method

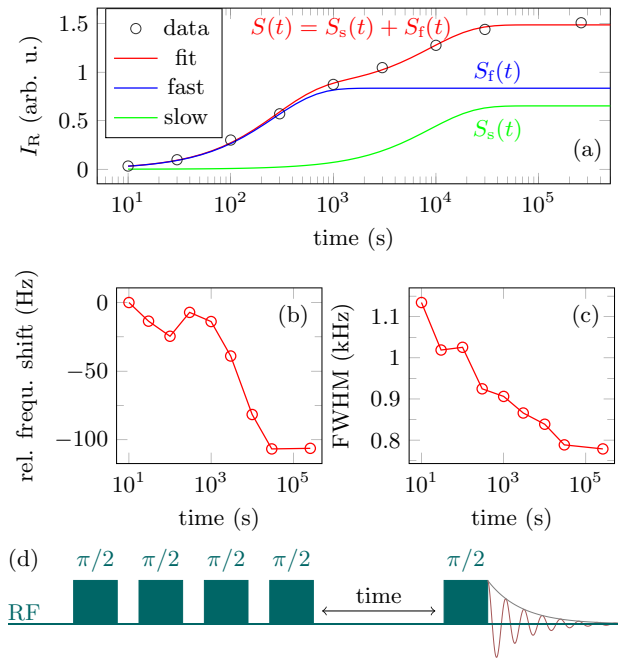


Figure 6. (a) NMR signal (integrated real part of the Fourier transform I_R) for different times after saturation at 11.74 T. The fitting parameters are: $T_1^f = 263(24)$ s, $T_1^s = 8700(1300)$ s with the ratio $A_s/A_f \approx 0.8$. A shift in the center frequency (b) as well as a narrowing of the NMR peaks (c) with increasing time is clearly visible. (d) Pulse sequence that was used with four $\pi/2$ pulses for saturation.

of CR is based on weakly coupled nuclear spins and induces spin diffusion. This is discussed further in the following section.

Magnetic field dependence

First of all, the distance of 0.114 mT of each peak pair of the magnetic field sweep corresponds to a coupling of the ^{13}C spins in the range of 2 MHz [10, 11]. At this point, it is unclear if this is intrinsically caused by the hyperpolarization process or can be explained by statistical arguments. Since the strongly coupled ^{13}C spins in the first shells around the paramagnetic center have a lower probability of occurrence. The first shell hyperfine (hf) coupling parameters for a NV center in the principal axis system are $A_{xx} = 30$ MHz, $A_{yy} = 123$ MHz and $A_{zz} = 227$ MHz [12]. Therefore, this coupling can not explain the experimental data. In [13] it was found experimentally as well as verified by theoretical *ab initio* calculations, that a NV- ^{13}C hf coupling around 2.5 MHz can be associated with 9 possible sites in a distance of 5 Å. In [14] couplings even below 1 MHz are reported. For P1 centers hf couplings with ^{13}C spins between 341 MHz and 1 MHz depending on the lattice site are reported [15–17]. Hence, the assumed hf coupling of ~ 2 MHz between the regarded paramagnetic centers and a ^{13}C spin is in accordance with the current literature.

Thermal measurements

Taking into account the double exponential decay as well as the narrowing of the line width in the QT measurements at 11.74 T, the ^{13}C spins can be separated at least in two groups.

The first one is located in the neighborhood of paramagnetic defects like NV or P1 centers (fast decay with $T_1^f = 4.4(4)$ min, broad line width) and the second group far away from any paramagnetic impurities (slow decay with $T_1^s = 2.0(4)$ h, narrow line width). Regarding the hyperpolarization decay at 7.05 T for short times, like shown in figure 3(a), no change in the NMR intensity in the range of $T_1^f \approx 4$ min is noticeable. Obviously, the main part of the hyperpolarized signal is contributed by ^{13}C beyond a minimal distance to the paramagnetic defects with long T_1 times. This is emphasized by the fact, that the line width of the hyperpolarized data is comparable with the QT measurements at 7.05 T only for long delay times in the latter (figure 5).

Spin diffusion

The dipolar echo experiment indicates a dipolar coupling among the hyperpolarized ^{13}C spins, which is a requirement for spin diffusion. But spin diffusion can take place only if the Larmor frequency of neighboring spins are in resonance. In the vicinity of a paramagnetic center a strongly magnetic field gradient is produced, inducing a shift of the nuclear Larmor frequency of the surrounding spins depending on their distance to the defect. This creates a diffusion barrier in the distance b around the defect. Within a radius $r < b$ the diffusion is suppressed (diffusion constant $D = 0$). The increase of D to its unperturbed value can be described by $\exp[-(b/r)^8]$ [18]. Assuming a hf coupling of ~ 2 MHz for NV- ^{13}C and extracting the NV- ^{13}C distance from [13] results in $b = 5\text{Å}$. The nuclear hf coupling with P1 centers is highly anisotropic but for a distance of 2.6 Å values from 1 MHz to 3 MHz are found [17]. Using the equation from [19] the diffusion barrier radius can be estimated with

$$b = \left(\frac{\hbar \gamma_e^2 B}{2k_B T \gamma_{13\text{C}}} \right)^{1/4} \cdot a$$

and gives $b = 3.2\text{Å}$ for the P1 center. This corresponds roughly to an exclusion of ^{13}C spins in the range of one lattice constant. Here, γ_e denotes the electronic gyromagnetic ratio, $\gamma_{13\text{C}}$ the ^{13}C gyromagnetic ratio, k_B the Boltzmann constant, T the temperature, B the external magnetic field and a the average nearest neighbor ^{13}C distance, with $T = 300$ K and $a = 4.4\text{Å}$. The parameter a is calculated via $1/2 = \exp\{-4\pi N_{13\text{C}} a^3/3\}$ to $a = 0.55 N_{13\text{C}}^{-1/3}$ [20]. This is depicted in the sketch of figure 8. For the NV center an additional region around the defect exists, where the strongly coupled ^{13}C spins get hyperpolarized directly via the excited state level anticrossing (ESLAC) in the investigated field region [21]. On the one hand this process seems to be less efficient for the bulk hyperpolarization and on the other hand this ESLAC polarized region overlaps at least partly with the diffusion barrier region.

The nuclear spin diffusion itself, shows a low diffusion constant $D = 67\text{Å}^2\text{s}^{-1}$ leading to a slow propagation and therefore a short spatial range (see supplemental material) [19]. However, the polarization in the order of several percent indicates a spread of the polarization over a wide region in the

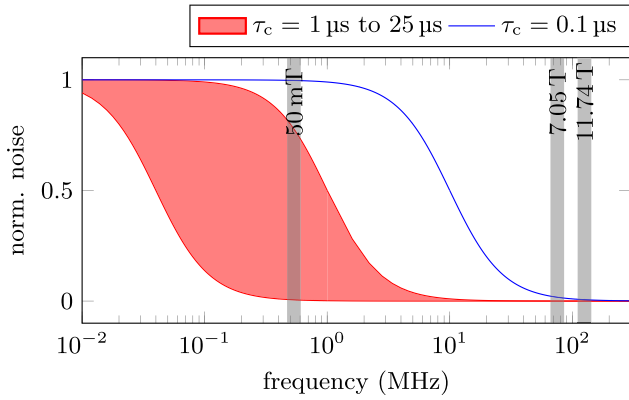


Figure 7. Normalized spectral noise density assuming an exponentially decaying auto correlation function for different correlation times τ_c . The gray regions indicate the ^{13}C Larmor frequencies for the three used magnetic fields of the presented measurements.

sample. This can not be explained by classical ^{13}C spin diffusion solely. An unknown effect seems to increase the diffusion range. We speculate that the diffusion enhancement is driven by the dipolar coupled P1 network.

Time dependence

The characteristic pumping time is at least roughly twice the decay time in the same field region. On the one hand, an unstable laser output in the first seconds can not be excluded, causing the longer pumping time. On the other hand, a reason for this could be the spread of the hyperpolarization over the bulk via diffusion and the fact, that the NV system is frequently in the excited state during the polarization. But the upper-state electronic configuration is different from that in the ground state, where the NV center is in resonance with the P1 defects.

Besides the ^{13}C spins, the NV centers as well as the coupled P1 centers are polarised during the laser illumination [22]. After switching off the laser light, the electronic spins of the paramagnetic centers decay quickly back into thermal equilibrium and induce magnetic noise which can influence the T_1 time of the nuclear ^{13}C spins. In the literature, the typical correlation times τ_c for magnetic noise around NV centers ranges from $1\ \mu\text{s}$ to $25\ \mu\text{s}$ [23–25]. For example, in [23] a $\tau_c = 3(2)\ \mu\text{s}$ for a nitrogen concentration of 100 ppm and a NV density of $10^{16}\ \text{cm}^{-2}$ were found. Assuming a Lorentzian spectral density for this noise, this can effect the relaxation times for the ^{13}C spins around 50 mT but not in the high field regime at 7.05 T and 11.74 T. Even a correlation time of $\tau_c = 0.1\ \mu\text{s}$ would have a low spectral density in the high field region (figure 7). Lower values of τ_c are reported for very impure systems like surface near NV centers in nanodiamonds [26]. A correlation time for the magnetic noise of $\tau_c > 0.1\ \mu\text{s}$ would explain the unchanged decay time of the hyperpolarization at the three measured low magnetic fields and the long relaxation time for high magnetic fields. For a

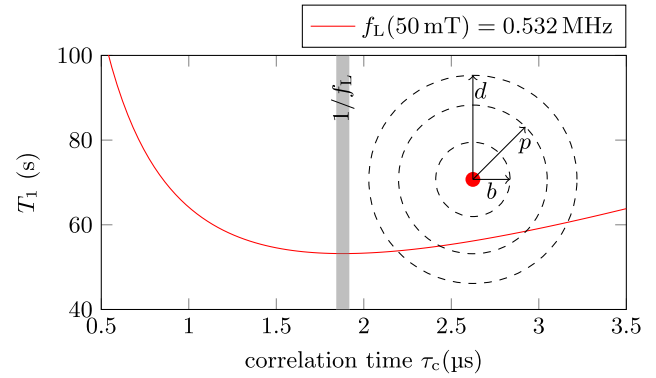


Figure 8. Dependence of the ^{13}C relaxation time T_1 from the correlation time τ_c . The vertical gray line indicates the Larmor period of ^{13}C spins in a magnetic field of around 50 mT. The red line corresponds to the equation (1) using a $\langle B_x^2 \rangle = 2 \times 10^{-4}\ \text{T}^2$. The inset depicts the different spheres around a paramagnetic defect (red). The parameter b denotes the characteristic radius of the diffusion barrier, p the radius for nuclear polarization via CR and d the diffusion radius.

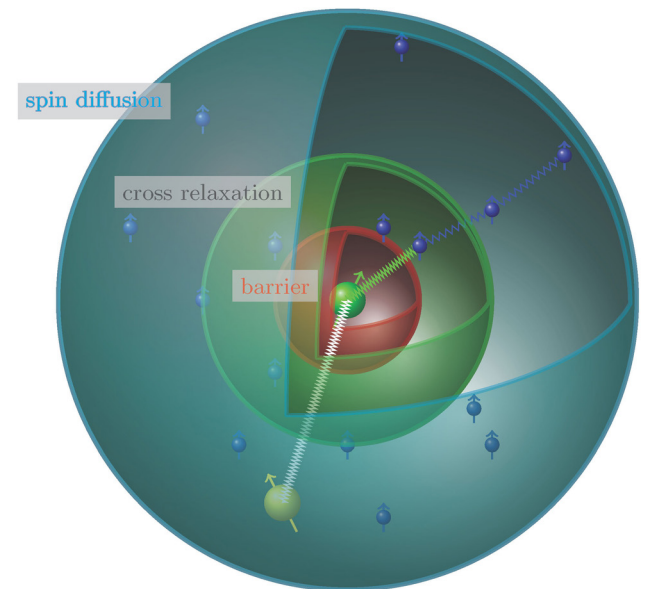


Figure 9. Sketch of the hyperpolarization mechanism in the picture of CR between a P1 and NV center (yellow and green spin). The defect is surrounded by a diffusion barrier (red) and a spherical shell of direct coupled ^{13}C spins (green). The electronic spin of one defect center is coupled to a nearby ^{13}C nuclear spin (blue spins), which leads to a polarization transfer to the latter. This polarization can diffuse in the bulk via the dipolar ^{13}C network. The range of spin diffusion is indicated by the outer sphere.

random fluctuating magnetic field B_x this can be modeled by the formula

$$\frac{1}{T_1} = \gamma_{13\text{C}} \langle B_x^2 \rangle \frac{\tau_c}{1 + (\omega_L \tau_c)^2}, \quad (1)$$

following from the theory of random fluctuating magnetic fields [27]. According to this equation, the previous reported correlation times around $3\ \mu\text{s}$ give reasons for the observed T_1 times in the low magnetic field region (figure 8).

Conclusion and outlook

Hyperpolarization measurements were compared with conventional measurements in QT equilibrium. The linewidth as well as the lattice relaxation times in both cases indicate a weak coupling to the directly hyperpolarized ^{13}C spins, an assertion that is supported by the magnetic field dependent hyperpolarization pattern.

Based on estimates for the radius of direct hyperpolarization via CR and the diffusion barrier, a scenario where the coupling between a NV and a P1 center leads to a polarization transfer to a nearby ^{13}C spin in a minimal distance beyond the diffusion barrier emerges, see figure 9. This polarization can be passed to the bulk ^{13}C spins via the dipolar network.

Further studies should also take into account an increasing range of effective spin diffusion with the aid of the network of coupled P1 centers. This could enhance the effective diffusion distance due to the stronger electronic dipolar coupling by a factor of $\gamma_{\text{P1}}/\gamma_{^{13}\text{C}} \approx 2600$.

Similar investigations of samples with varying defect concentrations could deliver valuable information of this hyperpolarization mechanism and open a way towards tailoring desired enhancement factors and relaxation times by defining the average defect distances.

Furthermore, the described method of hyperpolarization transfer should be applied on nano diamonds. This can open the opportunity to transfer the polarization out of the diamond to its surface.

Acknowledgments

This work was supported by the VolkswagenStiftung. We thank Dr W Knolle (Leibniz Institute of Surface Engineering (IOM), Leipzig, Germany) for helpful discussions and valuable assistance during the high energy electron irradiation. We acknowledge support from the German Research Foundation (DFG) and Leipzig University within the program of Open Access Publishing. Furthermore, we acknowledge support by P Racke in preparing the manuscript.

ORCID iDs

Ralf Wunderlich  <https://orcid.org/0000-0001-5841-6293>

References

- [1] Jacques V, Neumann P, Beck J, Markham M, Twitchen D, Meijer J, Kaiser F, Balasubramanian G, Jelezko F and Wrachtrup J 2009 *Phys. Rev. Lett.* **102** 057403
- [2] Wang H J, Shin C S, Avalos C E, Seltzer S J, Budker D, Pines A and Bajaj V S 2013 *Nat. Commun.* **4** 1940
- [3] Fischer R, Jarmola A, Kehayias P and Budker D 2013 *Phys. Rev. B* **87** 125207
- [4] King J P, Jeong K, Vassiliou C C, Shin C S, Page R H, Avalos C E, Wang H J and Pines A 2015 *Nat. Commun.* **6** 8965
- [5] Alvarez G A, Bretschneider C O, Fischer R, London P, Kanda H, Onoda S, Isoya J, Gershoni D and Frydman L 2015 *Nat. Commun.* **6** 8456
- [6] Ivady V, Szasz K, Falk A L, Klimov P V, Christle D J, Janzen E, Abrikosov I A, Awschalom D D and Gali A 2015 *Phys. Rev. B* **92** 115206
- [7] Yang P, Plenio M B and Cai J 2016 *EPJ Quantum Tech.* **3** 1
- [8] Scheuer J et al 2016 *New J. Phys.* **18** 013040
- [9] Fernandez-Acebal P et al 2018 *Nano Lett.* **18** 1882
- [10] Wunderlich R, Kohlrautz J, Abel B, Haase J and Meijer J 2017 *Phys. Rev. B* **96** 220407
- [11] Pagliero D et al 2018 *Phys. Rev. B* **97** 024422
- [12] Shim J, Nowak B, Niemeyer I, Zhang J, Brandao F and Suter D 2013 arxiv:1307.0257
- [13] Smeltzer B, Childress L and Gali A 2011 *New J. Phys.* **13** 025021
- [14] Dreau A, Maze J-R, Lesik M, Roch J-F and Jacques V 2012 *Phys. Rev. B* **85** 134107
- [15] Barklie R C and Guven J 1981 *J. Phys. C: Solid State Phys.* **14** 3621
- [16] Cox A, Newton M E and Baker J M 1994 *J. Phys.: Condens. Matter* **6** 551
- [17] Peaker C, Atumi M, Goss J, Briddon P, Horsfall A, Rayson M and Jones R 2016 *Diam. Relat. Mater.* **70** 118
- [18] Khutsishvili G R 1966 *Sov. Phys.—Usp.* **8** 743
- [19] Reynhardt E and High G 2001 *Prog. Nucl. Magn. Reson. Spectrosc.* **38** 37
- [20] Smeltzer B, McIntyre J and Childress L 2009 *Phys. Rev. A* **80**
- [21] Terblanche C, Reynhardt E C and van Wyk J A 2001 *Solid State Nucl. Magn. Reson.* **20** 1
- [22] Loretz M, Takahashi H, Segawa T F, Boss J M and Degen C L 2017 *Phys. Rev. B* **95** 064413
- [23] Bar-Gill N, Pham L, Belthangady C, Le Sage D, Cappellaro P, Maze J, Lukin M, Yacoby A and Walsworth R 2012 *Nat. Commun.* **3** 858
- [24] Wang Z H, de Lange G, Riste D, Hanson R and Dobrovitski V V 2012 *Phys. Rev. B* **85** 155204
- [25] de Lange G, van der Sar T, Blok M, Wang Z H, Dobrovitski V and Hanson R 2012 *Sci. Rep.* **2** 382
- [26] Song X, Zhang J, Feng F, Wang J, Zhang W, Lou L, Zhu W and Wang G 2014 *AIP Adv.* **4** 047103
- [27] Levitt M H 2009 *Spin Dynamics-Basics of Nuclear Magnetic Resonance* (New York: Wiley)